

An MP-DWR method for h-adaptive finite element methods

Chengyu Liu¹ and Guanghui Hu^{1,2,3*}

¹Department of Mathematics, Faculty of Science and Technology,
University of Macau, Macao SAR, China..

²Zhuhai UM Science & Technology Research Institute, Zhuhai,
Guangdong, China..

³Guangdong-Hong Kong-Macao Joint Laboratory for
Data-Driven Fluid Mechanics and Engineering Applications,
University of Macau, Macao SAR, China..

*Corresponding author(s). E-mail(s): garyhu@um.edu.mo;
Contributing authors: cyliu3551@gmail.com;

Abstract

In a dual weighted residual based adaptive finite element method for solving partial differential equations, a new finite element space needs to be built for solving the dual problem, due to the Galerkin orthogonality. Two popular approaches in the literature are ***h***-refinement and ***p***-refinement for the purpose, respectively, which would cause nonignorable requirement on computational resources. In this paper, a novel approach is proposed for implementing the dual weighted residual method through a multiple precision technique, i.e., the primal and dual problems are solved in two finite element spaces, respectively, built with the same mesh, degrees of freedom, and basis functions, yet different precisions. The feasibility of such an approach is discussed in detail. Besides effectively avoiding the issue introduced by the Galerkin orthogonality, remarkable benefits can also be expected for the efficiency from this new approach, since i). operations on reorganizing mesh grids and/or degrees of freedom in building a finite element space in ***h***- and ***p***-refinement methods can be avoided, and ii). both CPU time and storage needed for solving the derived system of linear equations can be significantly reduced compared with ***h***- and ***p***-refinement methods. In coding the algorithm with a library AFEPack, no extra module is needed compared with the program for solving the primal problem with the employment of a C++

feature *template*, based on which the floating point precision is used as a parameter of the template. A number of numerical experiments show the effectiveness and improvement for the efficiency of our method. Further discussion towards the limitation of the method is also delivered.

Keywords: finite element method; h-adaptive mesh method; dual-weighted residual; multiple precision; C++ template

1 Introduction

The adaptive finite element method is an efficient technique in computational science for improving the accuracy with an economical mesh, which has been used in many applications [1–3]. To implement numerical simulations of adaptive finite element methods, there have been various classic *a posteriori* error estimates such as residual estimates, hierarchical error estimates, and average methods. We refer to [4] for a comprehensive introduction.

In [5, 6], Becker and Rannacher proposed the dual weighted residual (DWR) method, which has the goal-orientation property. Thus, the DWR method can be applied to deal with the specified quantities in numerical simulations, from the the drag and lift coefficients of some objects in viscous flow[7] to some observable based on the time-dependent Schrödinger equation[8]. Different from the above classic methods such as residual type *a posteriori* error estimation which focuses on the error between the exact solution u and its approximation u_h , e.g., $\|u - u_h\|$, the DWR method has the capability of estimating the error between an exact quantity of interest $J(u)$ and its approximation $J(u_h)$, e.g., $\|J(u) - J(u_h)\|$.

In DWR, such an estimation is obtained through solving an auxiliary dual problem. The idea can be summarized based on a Poisson equation as follows. First of all, the Poisson equation is given by

$$\begin{cases} -\Delta u = f, & \text{in } \Omega, \\ u = 0, & \text{on } \partial\Omega, \end{cases} \quad (1)$$

where the unknown u and f are two functions defined on the domain Ω , and we consider a homogeneous Dirichlet boundary condition on the boundary $\partial\Omega$ for the well posedness. In a standard implementation of finite element method, a partition \mathcal{T} of the domain Ω needs to be generated first, based on which a finite element space $V_h \subset V$ can be built, where the space $V := H_0^1(\Omega) := \{v \in H^1(\Omega) : v|_{\partial\Omega} = 0\}$ with $H^1(\Omega)$ a standard Sobolev space. Then the task becomes finding an approximation $u_h \in V_h$ through solving the weak equation

$$a(u_h, v) := \sum_{K \in \mathcal{T}} \int_K \nabla u_h \cdot \nabla v = \sum_{K \in \mathcal{T}} \int_K f v = (f, v), \quad \forall v \in V_h. \quad (2)$$

It is well known that the residual type *a posteriori* error estimation is given by

$$C_2(\sum_K \eta_K^2)^{\frac{1}{2}} \leq \|u - u_h\| \leq C_1(\sum_K \eta_K^2)^{\frac{1}{2}}, \quad (3)$$

where C_1 and C_2 are positive constants, and η_K represents certain error indicator in the mesh element K .

To derive an error between $J(u)$ and $J(u_h)$, in the DWR framework we need to introduce an auxiliary dual problem

$$a(v, w) = J(v), \quad \forall v \in V, \quad (4)$$

where $J(\cdot)$ is assumed here to be a linear functional. Then a simple derivation gives

$$|J(u) - J(u_h)| = |J(u - u_h)| = |a(u - u_h, w)| \leq C\|u - u_h\|\|w\|. \quad (5)$$

With a residual type estimation of $\|u - u_h\|$ and an approximation \tilde{w} for w , the right hand side gives us a so-called *dual weighted residual* error estimation of $J(u) - J(u_h)$. It can be seen from the above discussion, finding the approximation \tilde{w} is the only left issue to deliver a quantized error estimation. It is noted that \tilde{w} need to be calculated from a space different from V_h , due to the Galerkin Orthogonality $a(u - u_h, v) = 0, \forall v \in V_h$, which results in the following two classical approaches [9]

- By h -refinement: the new space is built on a mesh generated from refining the original mesh, and
- By p -refinement: the new space is built by introducing more degrees of freedom into the original mesh.

Although the above two approaches are different with each other from the implementation point of view, they follow the same framework, i.e., a larger finite element space needs to be built first, then the dual problem (4) will be discretized in this space, and the derived larger system of linear equations will be solved for the dual solution. In the above framework, it can be seen that following the operations would be necessary, i.e., re-meshing, re-organizing the degrees of freedom, regeneration of the information of numerical quadrature, reformation of stiff matrix, and solving an even much larger system of linear equations. It is noted that to avoid the Galerkin orthogonality, an approximation \tilde{w} of w from a smaller finite element space can also be employed for the purpose, as mentioned in [10]. However, the operations mentioned above are still needed with classical approaches. In this work, we explore the possibility of building a different finite element space through one feature of the computer, i.e., finite precision arithmetic.

A key observation is that when the finite element space V_h is expressed in different floating point precisions, they should be two different finite element spaces from the computer point of view, even both spaces are built with the

4 An MP-DWR method for h -adaptive finite element methods

same configuration (same mesh, degrees of freedom, basis functions, etc). To understand it, we need to recall the way a real number is expressed in the computer. It is known that from IEEE standard shown in Fig. 1, each real number takes up 64 bits in double-precision formats, 32 bits in float-precision formats, and 16 bits in half-precision, respectively. Based on this, the same number stored with different precisions will behave differently in calculations.

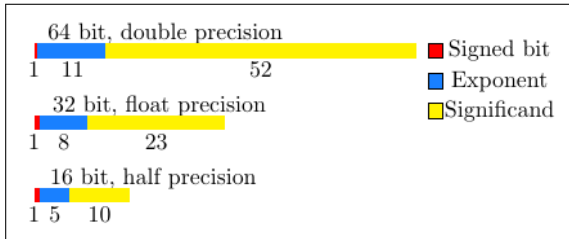


Fig. 1 IEEE754 data format

Hence, if we take two vectors $\vec{v}_1 = (\cos \frac{\pi}{3}, \sin \frac{\pi}{3})$ and $\vec{v}_2 = (-\sin \frac{\pi}{3}, \cos \frac{\pi}{3})$ as an example, it can be seen that two vectors are orthogonal with each other mathematically. Numerically, if two vectors are expressed in single-precision, the inner product (u, v) is computed as 0.00000000. We kept 8 digits after the decimal point which approaches the limit of single-precision. However, if v_1 is in single, and v_2 is in double, then the inner product becomes -0.000000007771812, which is obviously not zero in double-precision. Such an observation motivates an idea for the implementation of DWR, i.e., solving primal and dual problems in two different precisions to avoid the Galerkin orthogonality.

In this paper, a multiple precision DWR (MP-DWR) method is proposed for the implementation of h -adaptive finite element methods, towards improving the simulation efficiency. With the assumption that the primal problem is solved with single-precision and dual problem is solved with double-precision, the flowchart of the method can be summarized as follows. First of all, let V_h^f denotes the finite element space built on the partition \mathcal{T} of the domain Ω in single-precision, on which numerical solution u_h^f and corresponding error estimation are obtained by solving the primal problem (2). Then a new finite element space V_h^d is built on the same partition \mathcal{T} in double-precision, on which the dual solution w_h^d is obtained by solving a discrete dual problem derived from (4). Then from (5) a DWR *a posteriori* error estimation can be generated to serve the following local refinement of the mesh grids in the h -adaptive mesh method. The feasibility of above algorithm is discussed in detail in the paper, from which the break of the Galerkin orthogonality can be seen clearly from examples. The improvement for the efficiency can be expected from our method by observations that i). both the re-partitioning of mesh grids and the rearrangement of degree of freedoms as well as associate basis functions are avoided in our method, since neither h -refinement nor p -refinement is needed,

and ii). the involvement of single-precision calculation would bring the reduction of both CPU time and storage, in operations such as formation of stiff matrix and solving the derived system of linear equations. In numerical experiments, the significant acceleration by our method can be seen clearly, e.g., in solving 3D Poisson equation, around an order of magnitude difference of CPU time between an h -refinement strategy and our method can be observed in solving the dual problem for a 3D Poisson equation.

Another feature of our MP-DWR method is its concise coding work with the aid of *template* property in C++ language. In this paper, all simulations are realized by using a C++ library *AFEPack*[11], in which the code is organized following a standard procedure on solving partial differential equations, i.e., partitioning the domain, building a finite element space, forming a system of linear equations, imposing boundary conditions, as well as solving the system of linear equations. More importantly, each step in above procedure is realized as a module in *AFEPack*. It is recalled that in our MP-DWR method, the above procedure needs to be implemented twice in order for solving the primal and dual problems with different precision, respectively. Consequently, using the feature *template* of the C++ language and using the type of the floating-point number as a parameter of the template class would be a perfect choice for coding the MP-DWR method, which makes the code concise and easily managed. It is noted that the code for our MP-DWR method can be downloaded from [12] for reference.

The outline of this paper is as follows: In Section 2, based on the Poisson equation, the idea of goal-orientation and the dual weighted residual method in h -adaptive finite element methods are briefly reviewed. In Section 3, we describe a novel DWR implementation based on multiple-precision in detail. In Section 4, a number of numerical experiments are implemented, from which the significant improvement on the efficiency of simulations by the MP-DWR method can be successfully observed, compared with traditional implementation of DWR method. Furthermore, several remarks are delivered towards the properties and limitation of MP-DWR method, based on our numerical experience. Finally, a conclusion is given in Section 5.

2 Poisson equation and DWR based h -adaptive mesh methods

In this section, based on the Poisson equation, a DWR based h -adaptive finite element method is reviewed briefly, as well as the associated classical theory.

2.1 Poisson equation and finite element discretization

Consider the Poisson equation (1), and $\Omega \subset \mathcal{R}^d$ is a bounded domain in 2 ($d = 2$) or 3 ($d = 3$) dimensional space. We choose the variational space $V = H_0^1(\Omega)$ to incorporate the homogeneous Dirichlet boundary condition.

The inner product of V is defined as

$$(u, v) = \int_{\Omega} uv d\vec{x}. \quad (6)$$

Then integration by parts yields the bilinear operator $a(\cdot, \cdot)$:

$$\begin{aligned} (f, v) &:= \int_{\Omega} f v d\vec{x} = \int_{\Omega} (-\Delta u) v d\vec{x} \\ &= \int_{\Omega} \nabla u \cdot \nabla v d\vec{x} - \int_{\partial\Omega} v \frac{\partial u}{\partial \vec{n}} ds \\ &= \int_{\Omega} \nabla u \cdot \nabla v d\vec{x} := a(u, v), \end{aligned} \quad (7)$$

where \vec{n} denotes the outward unit normal to $\partial\Omega$. The weak solution u to the Poisson equation can be characterized via the variational problem:

$$\text{Find } u \in V, \text{ such that } a(u, v) = (f, v), \forall v \in V. \quad (8)$$

To approximate the weak solution, a finite-dimensional subspace needs to be constructed in V . In finite element methods, such a subspace is also called finite element space. The essential part for constructing finite element space is the finite element, which is defined as [13, 14]:

Definition 1 Let

- (i) $\mathcal{K} \subseteq \mathcal{R}$ be a bounded closed set with nonempty interior and piecewise smooth boundary (the *element domain*),
- (ii) \mathcal{P} be a finite-dimensional space of functions on K (the space of *shape functions*) and
- (iii) $\mathcal{N} = \{N_1, N_2, \dots, N_k\}$ be a basis for \mathcal{P}' (the set of *nodal variables*).

Then $(\mathcal{K}, \mathcal{P}, \mathcal{N})$ is called a *finite element*.

And the corresponding nodal basis in the \mathcal{P} is defined as:

Definition 2 Let $(\mathcal{K}, \mathcal{P}, \mathcal{N})$ be a finite element. The basis $\phi_1, \phi_2, \dots, \phi_k$ of \mathcal{P} dual to \mathcal{N} (i.e. $N_i(\phi_j) = \delta_{ij}$) is called the *nodal basis* of \mathcal{P} .

Denote P_k by the set of polynomials of degree $\leq k$. Let K be a simplex in \mathcal{R}^d with vertices $z_i, i = 1, 2, \dots, d+1$, $\mathcal{P} = P_1$, and $\mathcal{N} = \{N_1, \dots, N_{d+1}\}$, where $N_i(v) = v(z_i)$, for any $v \in \mathcal{P}$. Then $(K, \mathcal{P}, \mathcal{N})$ is a linear finite element. Let the set $\{\phi_i : 1 \leq i \leq d+1\}$ be the nodal basis the linear finite element

$(K, \mathcal{P}, \mathcal{N})$, the corresponding local interpolant can be defined as

$$\mathcal{I}_K v := \sum_{i=1}^{d+1} N_i(v) \phi_i. \quad (9)$$

Then we can piece together the element domains $\{K_i\}$ to get a triangulation (or mesh) \mathcal{T} of the domain Ω , which is a partition of the domain Ω in $\mathcal{R}^d (d = 2, 3)$ into a finite collection of triangles (tetrahedrons) $\{K_i\}$ satisfying that:

- (i) $\text{int } K_i \cap \text{int } K_j = \emptyset$ if $i \neq j$,
- (ii) $\bigcup K_i = \bar{\Omega}$,
- (iii) no vertex of any triangle (tetrahedron) lies in the interior of an edge (a face or an edge) of another triangle (tetrahedron).

Based on the triangulation, we can introduce the finite element space $V_h \subset H_0^1(\Omega)$ as

$$V_h = \{v \in H_0^1(\Omega) : v|_K \in P_1, \forall K \in \mathcal{T}\}. \quad (10)$$

In V_h , the Ritz-Galerkin approximation to (8) can be expressed as:

$$\text{Find } u_h \in V_h, \text{ such that } a(u_h, v) = (f, v), \forall v \in V_h \subset V. \quad (11)$$

Assume the set $\{\phi_1, \dots, \phi_{N_{bas}}\}$ is the basis of the V_h , where N_{bas} denotes the dimension of the V_h . Replacing the v by ϕ_i , then the (11) is equivalent to

$$a(u_h, \phi_i) = f(u_h, \phi_i), \quad i = 1, \dots, N_{bas}. \quad (12)$$

In the V_h , u_h can be represented by the basis as

$$u_h = \sum_{i=1}^{N_{bas}} U_i \phi_i, \quad (13)$$

where U_i denotes the value of u at the i -th vertex on the \mathcal{T} .

Combining (11)-(13), we can obtain a matrix-vector form corresponding to $U = [U_1, U_2, \dots, U_{N_{bas}}]$, which is the matrix of the unknown vectors:

$$AU = F, A \in \mathcal{R}^{N_{bas} \times N_{bas}}, \quad U, F \in \mathcal{R}^{N_{bas}}, \quad (14)$$

where $A_{ij} = a(\phi_j, \phi_i), i, j = 1, 2, \dots, N_{bas}$, and $F_i = (f, \phi_i), i = 1, 2, \dots, N_{bas}$. By solving (14), we can get the numerical Galerkin approximation to u .

2.2 Goal-orientation and dual weighted residual

In this subsection, the classical residual type *a posteriori* error estimation is introduced first, then an introduction of a framework of a goal-oriented *a posteriori* error estimation based on DWR method follows.

8 *An MP-DWR method for h-adaptive finite element methods*

Denote the exact solution of (1) and (11) by u and u_h , respectively. Generally, the exact form of u is unknown so it is impossible to compute the error $e_h := u - u_h$. However, the error e_h is related to the residual as:

$$\begin{aligned} a(e_h, v) &= a(u - u_h, v) \\ &= \int_{\Omega} \nabla(u - u_h) \cdot \nabla v d\vec{x} \\ &= \int_{\Omega} f v + \int_{\Omega} \nabla u_h \cdot \nabla v d\vec{x} = \mathcal{R}(v), \quad \forall v \in V. \end{aligned} \quad (15)$$

Then integration by parts element-wise to transform \mathcal{R} as:

$$\mathcal{R}(v) = \sum_K \int_K (f + \Delta u_h) v d\vec{x} + \sum_E \int_E J_E [\vec{n}_e \cdot \nabla u_h] v ds, \quad (16)$$

where K and E represent elements and the edges of elements, respectively. And the J_E is the "jump" term as:

$$J_E(v)(x) = \lim_{t \rightarrow 0^+} v(x - t\vec{n}_E) - \lim_{t \rightarrow 0^+} v(x + t\vec{n}_E), \quad \forall x \in E, \quad (17)$$

which describes any piecewise continuous function across the interior edge E and \vec{n} denotes the unit normal vector on the interior boundary E .

Based on (16), a classic residual error indicator for every element $K \in \text{mesh } \mathcal{T}$ can be obtained as

$$\eta_K = \left\{ h_K^2 \|\bar{f}_K + \Delta u_h\|_K^2 + \frac{1}{2} \sum_{E \in \varepsilon_{K,\Omega}} h_E \|J_E(\vec{n} \cdot \nabla u_h)\|_E^2 \right\}^{\frac{1}{2}}, \quad (18)$$

where $\varepsilon_{K,\Omega}$ represents the set which contains all interior boundaries of element K , and \bar{f} represents the average of f on element E . What is more, there are two constants c^* and c_* , which only depend on the shape parameter of T , such that the estimates

$$\|\nabla(u - u_h)\| \leq c^* \left\{ \sum_{K \in \mathcal{T}} \eta_K^2 + \sum_{K \in \mathcal{T}} h_K^2 \|f - \bar{f}_K\|_K^2 \right\}^{\frac{1}{2}} \quad (19)$$

and

$$\eta_K \leq c_* \left\{ \|\nabla(u - u_h)\|_{\omega_K}^2 + \sum_{K' \subset \omega_K} h_{K'}^2 \|f - \bar{f}_{K'}\|_{K'}^2 \right\}^{\frac{1}{2}} \quad (20)$$

hold for all elements $K \in \mathcal{T}$. ω_K is defined as:

$$\omega_K = \bigcup_{\varepsilon_K \cap \varepsilon_{K'} \neq \emptyset} K', \quad (21)$$

where ε_K represents the set which contains all boundaries of element K [4]. Besides that, the bound of error $e = u - u_h$ can be obtained as [14, 15]:

$$C_2(\sum_K \eta_K^2)^{\frac{1}{2}} \leq \|u - u_h\| \leq C_1(\sum_K \eta_K^2)^{\frac{1}{2}}. \quad (22)$$

Combining (18)-(22), the error can be evaluated by using such an *a posteriori* error indicator based on the residual \mathcal{R} , which is computable from f and u_h . With the help of the *a posteriori* error indicator, the adapted mesh have the capability of catching the critical regions of the exact solution. On such an adapted mesh, numerical simulations will be implemented more efficiently.

Generally, in practical numerical simulations, the quantities of interest can be some functionals of the exact solution u . But the classic residual-based estimates mainly focus on the energy norm or L^2 norm of the problems. These norms are usually different from the quantities of interest. Thus, the classic residual-based error estimates are not a good choice for the adaptation strategy anymore. To fix this, we consider the goal-orientation adaptation strategy, in which some terms consisting of goals, i.e. quantities of interest, should be added to the error estimates.

The dual weighted residual method is one class of goal-orientation adaptation approaches, which can be briefly summarized as follows. We still consider the Poisson equation (1) with the finite element discretization as above. Assume $J(\cdot)$ is the target functional which is linear. And $J(\cdot)$ satisfies

$$a(v, w) = J(v), \quad \forall v \in V, \quad (23)$$

where $w \in V$ is the solution of the associated dual problem. With $\varphi_h \in V_h$, (23) can be represented as

$$a(\varphi_h, w_h) = J(\varphi_h), \quad \forall \varphi_h \in V_h, \quad (24)$$

where $w_h \in V_h$. Combining (23) and (24), we can get the target functional of e :

$$J(e) := J(u - u_h) = a(u - u_h, w). \quad (25)$$

Based on the Galerkin orthogonality,

$$a(u - u_h, v_h) = 0, \quad \forall v_h \in V_h. \quad (26)$$

Then (25) can be expressed as

$$J(e) = a(u - u_h, w) - a(u - u_h, w_h) = a(u - u_h, w - w_h). \quad (27)$$

Therefore, if the solution $w \in V_h$, $J(e)$ will always be equal to zero, which means no useful information for the error estimates can be obtained. Thus, the approximation of w should be computed from a different space than V_h .

Suppose that one approximation of w denoted as \tilde{w} has been obtained from a different space V'_h . Thus \tilde{w} will not preserve the Galerkin orthogonality in V_h . Replacing the w by \tilde{w} , (25) can be transformed as

$$\begin{aligned} J(e) &= a(u - u_h, \tilde{w}) = a(u, \tilde{w}) - a(u_h, \tilde{w}) \\ &= (f, \tilde{w}) - a(u_h, \tilde{w}) \\ &= \int_{\Omega} (f + \Delta u_h) \tilde{w} d\vec{x}. \end{aligned} \quad (28)$$

With above equations, it can be derived that:

$$\begin{aligned} |J(e)| &= \left| \int_{\Omega} (f + \Delta u_h) \tilde{w} d\vec{x} \right| \\ &\leq \|R_h\| \|\tilde{w}\|, \end{aligned} \quad (29)$$

where $R_h = f + \Delta u_h = -\Delta u + \Delta u_h$.

The product of $\|R_h\| \|\tilde{w}\|$ is the so-called dual weighted residual, in which $\|R_h\|$ can be replaced by the residual-based error estimate from the above discussion and $\|\tilde{w}\|$ is the weight given by the approximation. In the calculations of building the dual weighted residual indicator, the term associated with R_h can be computed based on the primal solution. Then the only left issue is to obtain the approximation \tilde{w} breaking the Galerkin orthogonality from a different space.

Suppose the numerical primal solution u_h has been computed from the space V_h on the mesh \mathcal{T}_h . In addition, the residual R_H has also been computed. Based on these, there are two main classic approaches for computing \tilde{w} as follows.

- By h -refinement: A denser mesh $\tilde{\mathcal{T}}_h$ can be constructed by globally refining the mesh \mathcal{T}_h . Based on $\tilde{\mathcal{T}}_h$, a different space \tilde{V}_h can be built. Then the dual solution \tilde{w} can be obtained from \tilde{V}_h , e.g.,

$$\text{Find } \tilde{w} \in \tilde{V}_h, \text{ whose mesh size is smaller than } h. \quad (30)$$

- By p -refinement: A finite element space $\tilde{V}_h^{(2)}$ with higher polynomial degree elements has to be constructed. From $\tilde{V}_h^{(2)}$, the dual solution \tilde{w} can be obtained, e.g.,

$$\text{Find } \tilde{w} \in \tilde{V}_h^{(2)}, \text{ whose polynomial order is higher than } V_h. \quad (31)$$

However, in practical computations, both of the above approaches cost massive computing resources[6]. They all build a different finite element space for solving the dual problem. In such a process, some operations would be necessary, i.e., remeshing the grid, re-organizing the degree of freedoms, regeneration of the information of numerical quadrature, the reformation of stiff

matrix, and solving an even larger linear system of linear equations. These operations would cost large CPU time and memory storage in calculations. Thus, we expect to propose an efficient approach that can avoid these operations to accelerate the process of computing the approximation to the dual solution w .

3 A novel DWR implementation based on multiple-precision

To build a different dual space without the operations mentioned above, multiple-precision is a possible option. Recall the property of precision format in the above discussion, the same data stored in different precisions are represented differently in value. Moreover, two mathematically orthogonal vectors would be non-orthogonal in calculations by using multiple precision.

Such an idea can be used to build the dual space that can break the Galerkin orthogonality for realizing the DWR method. To make sure this idea works, we will show how the multiple precision breaks the Galerkin orthogonality at first. Recall the Galerkin orthogonality

$$a(e_h, v) = a(u - u_h, v) = 0,$$

holds for all $v \in V_h$. Then we can take $v = u_h$ in the formula and get

$$a(u - u_h, u_h) = 0. \quad (32)$$

By using a different precision in the calculations, a different space V'_h can be built without changing the mesh grid. The new numerical solution u'_h is obtained from V'_h . Then based on the above idea, u_h and u'_h would be different. Moreover, it can be expected that the Galerkin orthogonality between them would not be preserved:

$$a(u - u_h, u'_h) \neq 0. \quad (33)$$

We use two examples to show the performance of multiple-precision on Galerkin orthogonality in numerical computations. In the following two examples, multiple-precision is implemented by using a combination of double and float precision.

We focus on the Poisson equation in 2-dimensional. First, we consider the exact function as Example 1 in $\Omega = [-1, 1]^2$:

Example 1

$$u = \sin(\pi x)\sin(2\pi y). \quad (34)$$

To compute the numerical solutions of the Poisson equation as (13), two different finite element spaces V_{double} and V_{float} are built with double and single precision, respectively. Based on such two spaces, the corresponding

numerical solutions u_{double} and u_{float} can be obtained. Then we compute the numerical results of $a(u - u_{double}, u_{double})$ and $a(u - u_{double}, u_{float})$ to check if (32) and (33) hold. Denote degrees of freedom as Dofs. The numerical results are shown in Table 1.

Table 1 Galerkin orthogonality in Example 1.

Dofs	L2 Error	$a(u - u_{double}, u_{double})$	$a(u - u_{double}, u_{float})$
385	4.470e-1	-5.035e-5	-8.117e-5
1473	1.136e-1	-1.579e-7	-5.103e-4
5761	2.854e-2	-6.596e-10	-2.202e-3
22785	7.143e-3	8.254e-11	-9.337e-3

To test the solution with singularity in the domain, we consider the following example.

Example 2

$$u = 50(1 - x^2)(1 - y^2)\exp(1 - y^{-4}). \quad (35)$$

Then we solve the numerical solutions as (13) on the same mesh grid with different precisions. And the numerical results of $a(u - u_{double}, u_{double})$ and $a(u - u_{double}, u_{float})$ are shown in Table 2.

Table 2 Galerkin orthogonality in Example 2.

Dofs	L2 Error	$a(u - u_{double}, u_{double})$	$a(u - u_{double}, u_{float})$
385	4.879e-2	-1.039e-8	-2.483e-6
1473	1.234e-2	-4.164e-11	-9.306e-6
5761	3.094e-3	6.610e-13	-5.054e-5
22785	7.742e-4	4.830e-13	-1.938e-4

Tables 1 and 2 demonstrate that: (1) In V_{double} , the value of bilinear form $a(u - u_{double}, u_{double})$ tends to zero as refining the mesh. That means the Galerkin orthogonality of u_{double} is preserved better. (2) The value of $a(u - u_{double}, u_{float})$ does not converge to zero in fact. And the residual even increases as the mesh size decreases. Such phenomena mean that the Galerkin orthogonality between u_{double} and u_{float} is broken numerically.

Remark 1 It is noted that if we increase the Dofs continuously, the value of $a(u - u_{double}, u_{double})$ will tend to zero while $a(u - u_{double}, u_{float})$ will obviously be different from zero. Because with more degrees of freedom in computations, the numerical results will be more accurate. Then u_{double} will preserve Galerkin orthogonality better so $a(u - u_{double}, u_{double})$ will get closer to zero. On the contrary, u_{float}

will also be more accurate while it will break Galerkin orthogonality more obviously in theory. As a result, the value of $a(u - u_{double}, u_{float})$ will become further from zero.

From the above discussion, it is verified that the Galerkin orthogonality will not be preserved when the multiple-precision is used. It means that the dual solutions from the finite element space constructed with different precision will work in the DWR approach. Thus, by solving primal and dual problems in two different precision, the Galerkin orthogonality can be avoided. Based on this, we propose Algorithm 1 for the multiple-precision implementation of the DWR method.

Algorithm 1 Framework of Adaptive finite element method based on MP-DWR method.

Require: The initial mesh, \mathcal{T}_0 ; The tolerance of the error functional, tol ; The maximum iteration times, Max_{iter} ; the iteration times $k = 0$.

- 1: Build a finite element space V_h on the mesh \mathcal{T}_k ;
- 2: Compute the primal solution u_{float} in float-precision;
- 3: Compute the error $J(e)$.
- 4: If the error $J(e) \leq tol$ or $k > Max_{iter}$, stop;
- 5: Compute the dual solution w_{double} in double-precision;
- 6: Combine u_{float} and w_{double} to produce the error indicator η_{DWR} to get the new mesh \mathcal{T}_{k+1} ;
- 7: Update the iteration times $k = k + 1$ and return to step 1.

In the k -th iteration of the MP-DWR method, firstly, we build a finite element space V_{float} on the mesh \mathcal{T}_k in float-precision. Then the primal solution u_{float} can be obtained from V_{float} . And the residual-based error indicator can also be computed. Based on these, we can compute the $J(e)$. If $J(e)$ satisfies the tolerance, the iterations can be finished otherwise the calculation continues. By changing the precision of computations to double-precision, the dual solution w_{double} can be obtained on the same mesh grid. Then we can combine u_{float} and w_{double} to obtain the DWR error indicator η_{DWR} . Based on η_{DWR} , we can adapt \mathcal{T}_k to \mathcal{T}_{k+1} for the next iteration.

The advantages of our method can be described as follows. First of all, many repeated operations of building finite element space can be avoided. Compared with the two classic methods, the MP-DWR method only computes the modules of building the finite element space once in one iteration. With the help of multiple-precision, the re-partitioning of the mesh grid, the rearrangement of degrees of freedom, the recalculation of the quadrature information, the reformation of stiff matrix, and solving an even larger linear system of linear equations can be avoided in the process of obtaining the dual solution. Without these operations, significant improvements in efficiency can be obtained.

The second advantage of MP-DWR comes from the involvement of computations with low precision. On computers, if one number is stored in double-precision, it will cost 8 bytes. While it costs 4 bytes in single-precision. Thus, when a quantity of data is stored on computers in single-precision instead of double-precision, the storage memory will be saved by fifty percent. Besides that, data with lower precision is more conducive to accelerating the calculation. Consider following C++ codes:

```
double double_data = 0.;
for(int i = 0; i < 1.0e7; i++)
{ double_data += 4.0*atan(1.0); }

float float_data = 0.;
for(int i = 0; i < 1.0e7; i++)
{ float_data += float(4.0*atan(1.0)); }
```

The same operation of the data is implemented 1.0e7 times with different precisions. The corresponding CPU times for the calculations of the above two modules are recorded in Table 3. It is obvious that the CPU time for the calculations in float-precision is much less than double-precision. Combining these two improvements of the lower precision, it can be expected that the calculations with single-precision can save CPU time and memory storage compared with double-precision. Therefore, the single-precision calculation part in the MP-DWR method can bring further reductions in both CPU time and storage.

Table 3 CPU time for different precision formats

Precision format	CPU seconds
double	4.010e-2
float	2.448e-2

In addition, the realization of the MP-DWR method can be very concise by using *template*. In this paper, we implement all simulations based on the *AFEPack* library. The code in the *AFEPack* library follows a standard procedure for solving partial differential equations. Furthermore, each step in the standard produce of implementing finite element method is realized as a module based on *template* in *AFEPack*. So it is quite trivial to utilize the modules to realize Algorithm 1. The multi-precision computations can be implemented by using the type of floating-point numbers as parameters of the modules. For example, consider the definition of the bilinear operator module in *AFEPack*:

```
BilinearOperator<DIM, value_type0 , value_type1 ,DOW,TDIM0,TDIM1,Number>{ ... }.
```

To change the precision of the numbers in `BilinearOperator`, we can just change the *template* parameter ‘Number’ in the definition. Such a property of the *AFEPack* makes it convenient for us to build finite element spaces with different precisions by merely changing some parameters of the *template* class in modules without repeating the entire code for each precision format, which makes the realization of codes for our method very concise.

4 Numerical experiments

In the following numerical simulations, we use the linear triangle template element for 2-dimensional cases and the tetrahedron template element for 3-dimensional cases, respectively. All of the initial meshes in the following cases are obtained by globally refining the template meshes several times. And the template meshes are shown in Figure 2. All numerical examples presented in this paper are developed by using the *AFEPack*[11] in C++, and the hardware is a DELL Precision T5610 workstation with 12 CPU Cores and 64 Gigabytes memory.

Moreover, a high order Gaussian Quadrature is needed in the calculations. Higher order Gaussian Quadrature can produce more accurate results, which can break the Galerkin orthogonality more obviously as mentioned in Remark 1. Therefore, the MP-DWR error indicators can be more effective to capture the critical area of the quantities of interest.

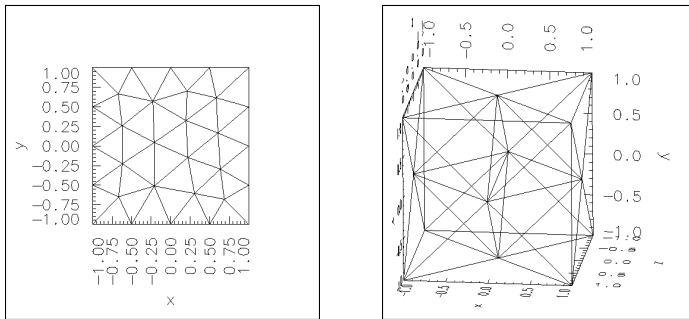


Fig. 2 Template mesh. Left: 2D case. Right: 3D case.

We focus on the *Poisson equation* in the following numerical examples. Based on it, a series of experiments are designed to test the effectiveness and the acceleration of our MP-DWR method. First of all, we would demonstrate the effectiveness of our method.

4.1 Effectiveness of MP-DWR method

To show the effect of mesh adaptation clearly, we use two-dimensional cases in this part. For the following examples, the domain is set as: $\Omega = [-1, 1]^2$.

Example 3 Set the exact u as:

$$u_1 := (1 - x^2)^2(1 - y^2)^2(kx^2 + 0.1)^{-1}, \quad (36)$$

where the k is set as 4, which represents the strength of the anisotropy[7].

The exact solution is shown in Figure 3 (Left). The target functional J of u_1 is defined as:

$$J_1(u) := |\Omega|^{-1} \int_{\Omega} u \, dp, \quad p = (x, y) \in \Omega. \quad (37)$$

We globally refine the mesh in Figure 2(Left) twice to obtain the initial mesh, on which we solve the Poisson equation with target functional J_1 through Algorithm 1. In addition, we reduce the adaptation tolerance in each iteration to test the effectiveness of Algorithm 1. An adapted mesh in the iterations is shown as Figure 3 (Middle). The convergence of Algorithm 1 is shown in Figure 4 (Left).

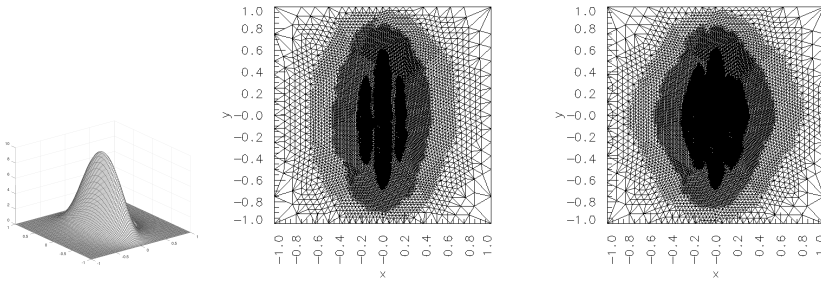


Fig. 3 The exact solution u_1 and the results of using MP-DWR in Example 3. Left: the exact solution u_1 ; Middle: an adapted mesh in the MP-DWR iterations associated with J_1 ; Right: an adapted mesh in the MP-DWR iterations associated with J_2

After that, we consider a different target functional J_2 of $u_1(x, y)$:

$$J_2(u) = |\Omega_2|^{-1} \int_{\Omega_2} u \, dp, \quad p = (x, y) \in \Omega_2, \quad (38)$$

where $\Omega_2 = [-1, 1] \times [-0.05, 0.05]$ is a small square domain. Then the operations same as above are implemented for the Poisson equation with J_2 . The

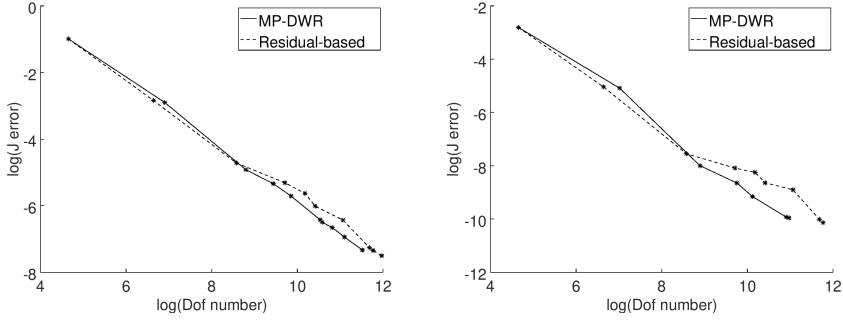


Fig. 4 The error of target functional obtained by MP-DWR method in Example 3 compared with the residual-based method. Left: J_1 error; Right: J_2 error.

corresponding numerical results are shown in figures (Figure 3, right; Figure 4, right).

From the above figures, two observations can be made, i.e., the convergence of our MP-DWR method that the error of the numerical solution decreases with the increment of mesh grids, and the advantage of our MP-DWR method compared with the residual-based method that much fewer mesh grids are needed to reach the same tolerance for the error.

To further confirm the effectiveness of MP-DWR, we consider a new function u_2 as in [7]:

Example 4

$$u_2 = 50(1 - x^2)(1 - y^2)\exp(1 - y^{-4}), \Omega = [-1, 1]^2. \quad (39)$$

First, we still set the associated target functional as $J_1(u)$ in (37). The exact solution of u_2 is plotted in Figure 5(Left).

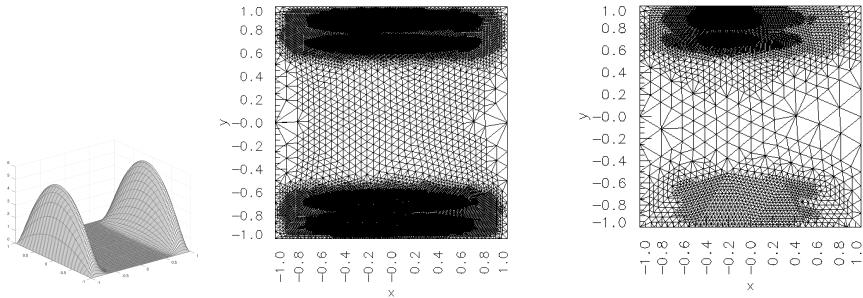


Fig. 5 The exact solution u_2 and the results of using MP-DWR in Example 4. Left: the exact solution u_2 ; Middle: an adapted mesh in the MP-DWR iterations associated with J_1 ; Right: an adapted mesh in the MP-DWR iterations associated with J_3

We globally refine the 2D-template mesh twice to obtain the initial mesh. After that, we refine the mesh based on the MP-DWR error indicator until the functional error $J(e)$ satisfies the tolerance. In addition, we reduce the adaptation tolerance in each iteration to check the convergence. The adapted mesh and the errors of the target functional are shown in Figure 5 (Middle) and Figure 6 (Left), respectively.

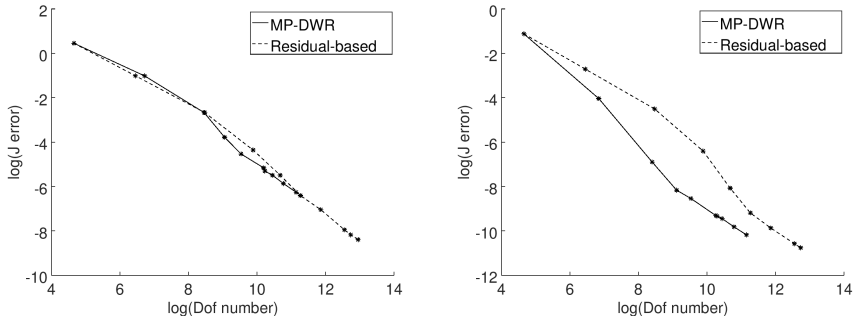


Fig. 6 The error of target functional obtained by MP-DWR method in Example 4 compared with the residual-based method. Left: J_1 error; Right: J_3 error.

After that, we consider a more special target functional J_3 for Example 4:

$$J_3(u) = |\Omega_3|^{-1} \int_{\Omega_3} u dp, \quad p = (x, y) \in \Omega_3, \quad (40)$$

where $\Omega_3 = [-0.5, 0] \times [0.7, 1]$. The domain Ω_3 is different from Ω_2 , which makes the target functional have different influences on the mesh adaptation. Then we implement the same operations as above for solving the Poisson equation based on the MP-DWR method. The numerical results are shown in figures (Figure 5 right; Figure 6 right).

In numerical experiments of Example 4, it is noted that the error $J(e)$ corresponding with J_1 or J_3 decreases as more degrees of freedom are added to the mesh grid, which demonstrates the convergence of the MP-DWR method. But in the situation with the target functional $J_1(u)$, the MP-DWR method shows similar convergence to the classic residual-based error estimate method. The reason might be that the interested domain of $J_1(u)$ is the whole domain Ω , in which the MP-DWR error indicator would be dominated by the residual-based term. However, in the situation with the target functional $J_3(u)$ focusing on the area $[-0.5, 0] \times [0.7, 1.0]$, around which the adapted mesh is much denser. Thus the MP-DWR method can catch the critical interesting area accurately. Besides that, our MP-DWR method uses much fewer degrees of freedom than the residual-based method to get a $J(e)$ reaching the same tolerance.

Combining the numerical results of Examples 3 and 4, the convergence of the MP-DWR method has been demonstrated. Furthermore, the MP-DWR

method generally requires much fewer mesh grids compared with the residual-based error indicator to obtain the $J(e)$ reaching the same tolerance. Thus, the effectiveness of our MP-DWR method can be verified. Then we will focus on the acceleration of the MP-DWR method.

4.2 Performance on acceleration

To illustrate the performance on acceleration, we compare the efficiency of our MP-DWR method with two main classic approaches (30) and (31). For simplicity, we denote the h -refinement and p -refinement approaches as Approach 1 and 2, respectively. In numerical simulations, we consider the following modules.

First of all, compare the CPU time taken in the error indicator generation part. The difference between the MP-DWR method and the classic approaches in the generation of the error indicator mainly focuses on two steps: solving the dual problem and building a dual weighted residual error indicator. Therefore, in the calculation, we only record the CPU time of these two steps in the first iteration. By comparing the recorded CPU time of the three approaches, we can verify the acceleration of our MP-DWR method.

In the numerical simulations, we still consider the Poisson equation with the exact solution as Example 3 (36). To make the comparison convincing, a series of different initial meshes are used in the numerical simulations. These initial meshes are obtained by globally refining the 2-dimensional template mesh as Figure 2 (Left) 2 to 5 times, on which the error indicators are obtained. CPU time and related data are recorded in the following Tables 4-7:

Table 4 2D case: CPU time needed in generating error indicator with 2nd h -refinement.

	Initial Dofs	Initial Elements	CPU seconds
Approach 1	385	704	7.607e-1
Approach 2	385	704	8.755e-1
MP-DWR	385	704	2.502e-1

Table 5 2D case: CPU time needed in generating error indicator with 3rd h -refinement.

	Initial Dofs	Initial Elements	CPU seconds
Approach 1	1473	2816	3.131e0
Approach 2	1473	2816	3.566e0
MP-DWR	1473	2816	0.871e0

Since many problems are applied in reality, numerical simulations implemented in 3-dimensional are more practical. Then we extend u_1 to a

Table 6 2D case: CPU time needed in generating error indicator with 4th h-refinement.

	Initial Dofs	Initial Elements	CPU seconds
Approach 1	5761	11264	1.208e1
Approach 2	5761	11264	1.378e1
MP-DWR	5761	11264	3.635e0

Table 7 2D case: CPU time needed in generating error indicator with 5th h-refinement.

	Initial Dofs	Initial Elements	CPU seconds
Approach 1	22785	45056	4.672e1
Approach 2	22785	45056	5.494e1
MP-DWR	22785	45056	1.401e1

3-dimensional situation. The 3-dimensional u_1 is expressed as

$$u_{1,3d} = \frac{(1-x^2)^2(1-y^2)^2(1-z^2)^2}{(kx^2+0.1)(ky^2+0.1)(kz^2+0.1)}, \quad (41)$$

where the parameter $k = 4$ determines the strength of the anisotropy, with the domain $\Omega = [-1, 1]^3$ and on the boundary $u_{\partial\Omega} = 0$. And we consider the average target functional:

$$J(u) := |\Omega|^{-1} \int_{\Omega} u \, dp, \quad p = (x, y, z) \in \Omega. \quad (42)$$

Similar to the above simulation, we implement the iteration once from the initial meshes to generate the error indicator through two classic approaches and the MP-DWR method, respectively. The initial meshes are obtained by globally refining the 3-dimensional template mesh as Figure 2 (Right) 2 to 5 times. Based on them, the error indicators are obtained from the first iteration. The CPU time and mesh information are provided in Tables 8, 9, 10 and 11.

As shown in the Tables 4-11, the MP-DWR method costs much less CPU time to obtain the error indicator than the two classic approaches. Therefore, it can be verified that MP-DWR tremendously accelerates the process of obtaining a dual weighted error indicator. Furthermore, the improvement of MP-DWR in CPU time becomes more significant when the problem size gets large, i.e., the number of degrees of freedom and elements is large.

Then we focus on the acceleration for the whole simulation. Unlike the above modules, we execute the iterations in Algorithm 1 until the numerical result reaches a specified level. The CPU time of the whole process is recorded for comparison.

In simulations, we consider the 3-dimensional Poisson equation with exact solution $u_{1,3d}$. Then the numerical solution is obtained based on Approach 1

Table 8 3D case: CPU time needed in generating error indicator with 2nd h -refinement.

	Initial Dofs	Initial Elements	CPU seconds
Approach 1	365	1536	2.9383e0
Approach 2	365	1536	3.4642e0
MP-DWR	365	1536	1.2679e-1

Table 9 3D case: CPU time needed in generating error indicator with 3rd h -refinement.

	Initial Dofs	Initial Elements	CPU seconds
Approach 1	2457	12288	2.2521e1
Approach 2	2457	12288	2.6414e1
MP-DWR	2457	12288	3.0338e0

Table 10 3D case: CPU time needed in generating error indicator with 4th h -refinement.

	Initial Dofs	Initial Elements	CPU seconds
Approach 1	17969	98304	1.7271e2
Approach 2	17969	98304	2.3313e2
MP-DWR	17969	98304	2.2336e1

and the MP-DWR method, respectively. The initial mesh is obtained by globally refining the 3-dimensional template mesh 2 to 4 times. The corresponding numerical results are shown in Tables 12, 13, 14. It can be observed that the MP-DWR method costs much less time than Approach 1 to obtain the result at a similar level. Such differences in CPU time demonstrate the acceleration of MP-DWR for the whole simulation. Besides that, the improvement in total CPU time becomes more obvious while the scale of the problem gets larger. In summary, our MP-DWR method shows significant improvement compared with the classic approach 1 in the whole adaptive finite element simulations.

Remark 2 To make these comparisons fair, we use the *AMGSolver* from *AFEPack* as the linear system solver in all numerical simulations. However, as a linear solver, *AMGSolver* may cost much time to solve the matrix-vector form 14 obtained from high order finite elements in Approach 2. Besides that, if the linear system solver for Approach 2 is changed, the new solver may have different numerical efficiency from *AMGSolver* which make the comparison unfair. Considering these factors, the part of solving the linear system in Approach 2 may hinder reasonable comparisons of CPU time. Therefore, when the comparison focuses on the acceleration for the whole simulation, we ignore Approach 2 to keep the comparison fair.

Remark 3 Besides that, due to the primal solution obtained in a lower precision format than the dual solution, it is necessary for us to compute the primal solution

Table 11 3D case: CPU time needed in generating error indicator with 5th h-refinement.

	Initial Dofs	Initial Elements	CPU seconds
Approach 1	137313	786432	1.409e3
Approach 2	137313	786432	1.898e3
MP-DWR	137313	786432	1.753e2

Table 12 3D case: CPU time needed in the whole simulation with 2nd h-refinement.

	Adapted Dofs	Adapted Elements	CPU seconds
Approach 1	17380	91206	7.864e2
MP-DWR	17388	91269	2.210e2

Table 13 3D case: CPU time needed in the whole simulation with 3rd h-refinement.

	Adapted Dofs	Adapted Elements	CPU seconds
Approach 1	18636	98549	9.465e2
MP-DWR	18497	97723	2.633e2

in the final mesh grid in higher precision (double) again. Such post-processing will cost a little more time. We record the CPU time in Table 15. As shown in Table 15, extra time is only about 10 percent of the whole CPU time for the whole simulation of MP-DWR. What is more, it is much smaller than the improvement of MP-DWR in CPU time. Thus, post-processing does not have much impact on the total efficiency, and the corresponding extra CPU time is also acceptable.

4.3 Changing the module of Algorithm 1

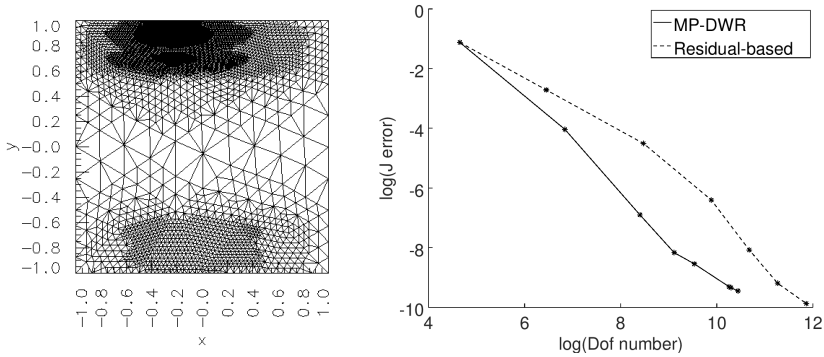
In previous numerical experiments, we compute primal solutions with single-precision and obtain dual solutions with double-precision in Algorithm 1. The reason is that we want to obtain an accurate dual solution closer to the exact value, which can make the dual weights more effective. But in numerical simulations, we can also compute primal solutions with double precision and obtain dual solutions with single precision to construct an effective dual weighted residual error indicator. To check the effectiveness of the new module, we perform an additional numerical simulation based on the Poisson equation. The exact solution is set as the the function (39) in Example 4 with the target functional J_3 (40). The initial mesh is obtained by globally refining the 2-dimensional template mesh twice, on which we solve the Poisson equation by using revised Algorithm 1. An adapted mesh in the numerical simulation is shown as Figure 7 (Left).

Table 14 3D case: CPU time needed in the whole simulation with 4th h -refinement.

	Adapted Dofs	Adapted Elements	CPU seconds
Approach 1	30133	163810	1.871e3
MP-DWR	30161	163978	5.006e2

Table 15 CPU time for post-processing

Approach 1	MP-DWR	Improvement	Post-processing
7.864e2	2.210e2	5.654e2	2.117e1
9.465e2	2.633e2	6.832e2	2.213e1
1.871e3	5.006e2	1.370e3	3.502e1

**Fig. 7** Results of the MP-DWR in the new module. Left: adapted mesh. Right: $J(e)$

The adapted mesh shows that the error indicator from revised MP-DWR can still catch the critical domain corresponding with the residual and target functional J_3 . Then we continue the iterations meanwhile reducing the adaptation tolerance in every iteration to test the convergence of the revised MP-DWR. As shown in Figure 7 (Right), the revised MP-DWR method obtains a more accurate result as the number of degrees of freedom increases, which confirms the convergence. More importantly, the revised MP-DWR method uses much fewer degrees of freedom compared with residual-based methods to obtain the numerical results reaching the same tolerance. Thus the effectiveness of the MP-DWR method with the new module can be verified. In addition, due to the primal solution obtained in double-precision, post-processing is not required in the new module, which can save a little time.

4.4 The limit of MP-DWR method

In some numerical experiments, it is strange that MP-DWR becomes less effective with refining the mesh too many times. Consider the Poisson equation

with the exact solution as (39) with target functional J_1 . We solve the numerical solution through MP-DWR and revised MP-DWR, respectively. In this way, the primal solution is obtained with double-precision and single-precision, respectively. Besides that, we set a very tiny adaptation tolerance in the simulations, which would make the mesh grid quite dense. The numerical results of the primal solutions obtained with double and float precision are shown in Figure 8. It can be seen that when the mesh grids are dense enough, the residual in single-precision increases as the number of degrees of freedom increases, which is different from the residual in double-precision. Moreover, such an inaccurate primal solution in single-precision can not construct a reliable dual weighted residual error indicator. One possible reason is that while we adapt

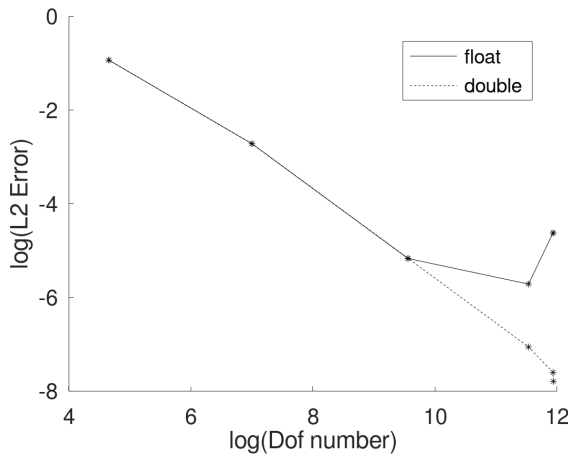


Fig. 8 Primal solutions computed in float and double precision.

the mesh several times, the number of degrees of freedom becomes large and the minimal volume of elements will get very tiny. For reference, the minimal volumes of elements on the mesh grids in each iteration are shown in Table 16. When the minimal volume gets the level of $1.0\text{e-}6$, the data will be close to the limit of single-precision so that the computations may demonstrate some unexpected phenomena causing the strange curve in Figure 8.

Table 16 The minimal volume of elements in adaptation

Adapt times	1	2	3	4	5
Minimal element volume	1.617e-2	1.010e-3	6.316e-05	4.34e-06	1.247e-06

Due to such a limit, we have to be careful about the data precision in numerical simulations while using MP-DWR methods, which means that we can not refine the mesh grids too many times, otherwise, the numerical results

would lose accuracy. Thus we suggest using the MP-DWR method as the preconditioned method for optimizing the mesh grids to make full use of the acceleration of the MP-DWR method and to avoid the above limit.

Remark 4 Although there is a limit to the MP-DWR method, we propose a potential algorithm to make full use of the advantages of the MP-DWR method: First, we can compute the primal solution with half-precision and dual solution with single-precision, respectively. When the primal solution gets the limit of half-precision, we change the precision parameters in our programming to compute the primal with single-precision and dual solution with double-precision, respectively. In this way, we can make full use of the acceleration of the MP-DWR method to get a reliable numerical result. And such an algorithm can also be an efficient preconditioned approach.

5 Conclusion

To accelerate the process of obtaining dual solution in the DWR methods, we utilize the properties of precision formats and propose a novel DWR implementation based on multiple-precision named MP-DWR. Numerical experiments confirm the effectiveness of the novel approach. Furthermore, it demonstrates obvious acceleration in computations compared with classic approaches. Although there is a limit to the MP-DWR method due to the property of precision formats in some situations, the substantial improvements in data storage and CPU time suggest that it is still an efficient method. Therefore, it has the potential to be an efficient pre-conditioned method. In future research, we expect to extend MP-DWR to solve some nonlinear model problems with error estimates in different forms.

Acknowledgement

The research of G. Hu was partially supported by National Natural Science Foundation of China (Grant Nos. 11922120 and 11871489), FDCT of Macao SAR (0082/2020/A2), MYRG of University of Macau (MYRG2020-00265-FST) and Guangdong-Hong Kong-Macao Joint Laboratory for Data-Driven Fluid Mechanics and Engineering Applications (2020B1212030001).

Statements and Declarations

Data availability statements

Data sharing not applicable to this article as no datasets were generated or analysed during the current study.

Competing interests

The authors declare that they have no conflict of interest.

References

- [1] Xu, F., Huang, Q., Chen, S., Ma, H.: A type of cascadic adaptive finite element method for eigenvalue problem. *ADVANCES IN APPLIED MATHEMATICS AND MECHANICS* **12**(3), 774–796 (2020)
- [2] Yang, L., Hu, G.: An adaptive finite element solver for demagnetization field calculation (2019)
- [3] Chen, Y., Huang, Y., Yi, N.: A decoupled energy stable adaptive finite element method for cahn–hilliard–navier–stokes equations. *Communications in Computational Physics* **29**(4), 1186–1212 (2021)
- [4] Verfürth, R.: *A Posteriori Error Estimation Techniques for Finite Element Methods*, OUP Oxford, 2013
- [5] Becker, R., Rannacher, R.: A feed-back approach to error control in finite element methods: Basic analysis and examples. *East-West Journal of Numerical Mathematics* **4** (1996)
- [6] Becker, R., Rannacher, R.: An optimal control approach to a posteriori error estimation in finite element methods. *Acta numerica* **10**, 1–102 (2001)
- [7] Wolfgang Bangerth, R.R.: *Adaptive Finite Element Methods for Differential Equations*. Birkhäuser Basel, November 2013
- [8] Kormann, K.: A time-space adaptive method for the schrödinger equation. *Communications in Computational Physics* **20**(1), 60–85 (2016)
- [9] Giles, M.B., Süli, E.: Adjoint methods for pdes: a posteriori error analysis and postprocessing by duality. *Acta numerica* **11**, 145–236 (2002)
- [10] Moon, K.-S., Szepessy, A., Tempone, R., Zouraris, G.E.: A variational principle for adaptive approximation of ordinary differential equations. *Numerische Mathematik* **96**(1), 131–152 (2003)
- [11] Li, R.: On multi-mesh h-adaptive methods. *Journal of Scientific Computing* **24**(3), 321–341 (2005)
- [12] <https://github.com/Mixed-DWR/MP-DWR.Example2.git>
- [13] Ciarlet, P.G.: Interpolation error estimates for the reduced hsieh-clough-tocher triangle. *Mathematics of Computation* **32**(142), 335–344 (1978)
- [14] Brenner, S.C., Scott, L.R., Scott, L.R.: *The Mathematical Theory of Finite Element Methods vol. 3*, Springer, 2008

- [15] Richter, T., Wick, T.: Variational localizations of the dual weighted residual estimator. *Journal of Computational and Applied Mathematics* **279**, 192–208 (2015)